Influence of convergence angle of tooth preparation on the fracture resistance of Y-TZP-based all-ceramic restorations

4 authors:

Pedro Henrique Corazza
Universidade de Passo Fundo
41 PUBLICATIONS 510 CITATIONS

SEE PROFILE

Sabrina Feitosa
IUSD
24 PUBLICATIONS 243 CITATIONS

SEE PROFILE

Alexandre Luiz Souto Borges
São Paulo State University
205 PUBLICATIONS 989 CITATIONS

SEE PROFILE

Alvaro Della Bona
Universidade de Passo Fundo
257 PUBLICATIONS 6,792 CITATIONS

SEE PROFILE

Some of the authors of this publication are also working on these related projects:

Project Brazilian Dental Science View project

Project Finite Element Analysis of dental materials and prosthodontics View project

Volume 29 Number 3 March 2013 ISSN 0109-5641

dental
materials

Journal for Oral and Craniofacial Biomaterials Sciences

www.demajournal.com

Available online at www.sciencedirect.com

SciVerse ScienceDirect

Official Publication of the Academy of Dental Materials

Influence of convergence angle of tooth preparation on the fracture resistance of Y-TZP-based all-ceramic restorations

Pedro Henrique Corazza[a], Sabrina Alves Feitosa[a], Alexandre Luiz Souto Borges[a], Alvaro Della Bona[b],*

[a] Department of Dental Materials and Prosthodontics, Sao Paulo State University – UNESP, Sao Jose dos Campos, SP, Brazil
[b] University of Passo Fundo, Dental School, Post-graduation Program in Dentistry, Passo Fundo, Brazil

ARTICLE INFO

ABSTRACT

Objective. To investigate the influence of the convergence angle of tooth preparation on the fracture load of Y-TZP-based ceramic (YZ – Vita YZ) substructure (SB) veneered with a feldspathic porcelain (VM9 – Vita VM9).

Methods. Finite element stress analysis (FEA) was performed to examine the stress distribution of the system. Eighty YZ SB were fabricated using a CAD–CAM system and divided into four groups ($n = 20$), according to the total occlusal convergence (TOC) angle: G6 – 6° TOC; G12 – 12° TOC; G20 – 20° TOC; and G20MOD – 20° TOC with modified SB. All SB were veneered with VM9, cemented in a fiber reinforced epoxy resin die, and loaded to failure. Half of the specimens from each group ($n = 10$) were cyclic fatigued (10^6 cycles) before testing. Failure analysis was performed to determine the fracture origin. Data were statistically analyzed using Anova and Tukey's tests ($\alpha = 0.05$).

Results. The greatest mean load to fracture value was found for the G20MOD, which was predicted by the FEA. Cyclic fatigue did not significantly affect the load of fracture. Catastrophic failure originating from the internal occlusal surface of the SB was the predominant failure mode, except for G20MOD.

Significance. The YZ–VM9 restorations resisted greater compression load than the usual physiological occlusal load, regardless of the TOC angle of preparations. Yet, the G20MOD design produced the best performance among the experimental conditions evaluated.

© 2013 Academy of Dental Materials. Published by Elsevier Ltd. All rights reserved.

1. Introduction

The introduction of high crystalline content ceramic materials increased the use of metal-free restorations. The yttria partially stabilized zirconia (Y-TZP) has aroused the greatest interest among the metal-free ceramic systems [1,2]. Several studies reported on the properties of Y-TZP ceramic [3–8], broadening clinical applications. However, the clinical success of these restorations is also dependent on other factors, such as tooth preparation and restoration design [9–12] that have shown little evolution over the time. Tooth preparation for prosthetic restorations was among the first aspects to receive specific recommendations. In 1923, Prothero indicated that the total occlusal convergence (TOC), which consists of the convergence angle between two opposing axial surfaces, should range from 2° to 5° [10]. The ideal TOC values are considered to be between 2° and 22° [10,13–15]. Nevertheless,

studies have shown the difficulty in obtaining preparations with low mean TOC values [16–19], which ranged from 14.1° [19] to 27.3° [16] varying according to the preparation purpose (extra-oral training or intra-oral practice), type and location of the tooth and dental surfaces involved. Yet, preparations with 12° TOC are recommended for metal-free crowns machined by CAD–CAM systems [20,21] mainly because of the marginal and internal adaptation resulting from this TOC.

The preparation TOC influences on the amount of restorative material required for the rehabilitation. It seems that the design and the amount of the porcelain and ceramic layers may influence the fracture resistance of the restoration, since these factors produce different stress distribution throughout the structure [11,12,22]. The few clinical studies on Y-TZP-based restorations reported that chipping failures are a significant problem of this system [23,24]. The ceramic–porcelain bond strength seems to be another inherent problem of zirconia-based restorations and may facilitate porcelain chipping [8,25].

Understanding the clinical failure mode of dental ceramics is crucial to adequate indication of such restorations. Principles of fractography are used to study the fracture surfaces of a ceramic restoration [2,8,11,12,26,27]. In an attempt to reproduce the clinical failure of brittle materials in laboratory experiments, some researchers [6,11,12,27,28] have developed innovative methodologies, identifying the fracture origin, which is usually located at porcelain subsurface [6] or at cementation surface [27].

Finite element analysis (FEA) is a useful tool for a non-destructive approach, since it has the ability to predict the mechanical and structural behavior of the materials, evaluating different designs, load types and elastic characteristics of the experimental components [29]. Thus, the purpose of this study was to investigate the influence of tooth preparation TOC and cyclic fatigue on the fracture load of Y-TZP-based ceramic substructure (SB) veneered with a feldspathic porcelain, testing the hypotheses that (1) the maximum principal stress varies according to the TOC angle of the FEA models, (2) the cyclic fatigue decreases the fracture load of the restorations, and (3) the preparation TOC angle and the SB design of the restorations influence the load to fracture.

2. Materials and methods

The materials used in this study are shown in Table 1.

2.1. Finite element analysis (FEA)

The stress distribution of ceramic restorations cemented on preparations with different TOC angles was investigated using FEA. The models simulated the experimental tests and had the following parameters: base of 8 mm (diameter) × 6 mm (height), preparation of 6 mm in height, rounded shoulder finish line (radius = 0.5 mm) and TOC angles varying according to the models (experimental groups). FEA models named G6,
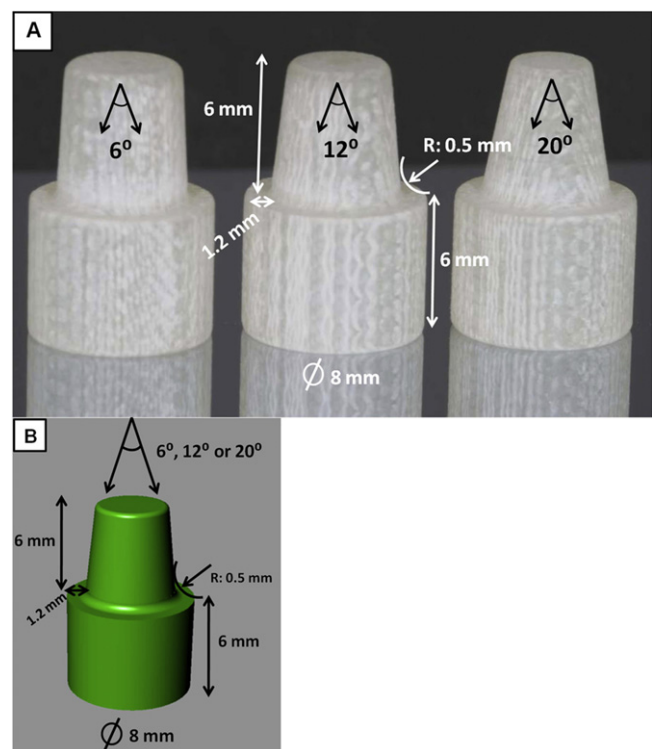

Fig. 1 – (A) Dies fabricated with the dentin analog material (NEMA grade G10). Preparations have 6°, 12° and 20° TOC angles. The 20° TOC die was used for groups G20 and G20MOD. (B) Same experimental parameters were applied to the FEA models.

G12 and G20 had preparations with 6°, 12° and 20° TOC angles, respectively (Fig. 1). The substructure (SB) thickness was uniform, 0.5 mm in the axial walls and 0.7 mm in the occlusal surface, for all three models (Fig. 2). The G20MOD model simulated a modified SB cemented on a 20° TOC preparation. The aim of the G20MOD modified SB was to compensate for the convergence angle, resulting in a porcelain layer similar to G6 model (Fig. 2). The cement thickness was set to 100 μm [30] for all models and the external design of the restorations was identical regardless of the TOC angle of the preparations. The models were created (Rhinoceros 4.0, Seattle, WA, USA) and exported to a simulation program (Ansys, Canonsburg, PA, USA), where the material properties were inserted (Table 2). It was assumed that all solids were homogeneous, isotropic and linear elastic. The components were considered perfectly bonded and flawless. A mesh composed by tetrahedral dominant elements was generated after the convergence test, which was done by changing the size of elements to reach less than 10% of variation. The number of nodes ranged between 509,226 (G20) and 548,382 (G6), and the number of elements were from 293,067 (G20) to 314,910 (G6). The support base was constrained in the three axes (x, y and z) and the stress was generated from a load of 1000 N applied to the center of the occlusal surface of the restoration (area of 0.03 mm^2) in the axial axis direction (Fig. 2). Maximum principal stress (MPS) analysis was used to verify the stress distribution in the materials.

Table 1 – Brand names, manufacturer and description of the materials.		
Brand name	Manufacturer	Description
VITA In-Ceram® YZ	Vita Zahnfabrik, Bad Sackingen, Germany	Densely sintered zirconia-based ceramic partially stabilized by yttria, indicated for bridge and crown substructures (CTE ≈ 10.5×10^{-6} K^{-1})
VITA VM®9	Vita Zahnfabrik, Bad Sackingen, Germany	Feldspathic porcelain indicated for veneer zirconia-based substructures (CTE ≈ 9×10^{-6} K^{-1})
VITA VM® Modeling Liquid	Vita Zahnfabrik, Bad Sackingen, Germany	Liquid indicated for mixing with the porcelain powder
VITA In-Ceram® YZ COLORING LIQUID (color LL1)	Vita Zahnfabrik, Bad Sackingen, Germany	Pigmented liquid used for complete or partial coloring of frameworks made from VITA In-Ceram YZ zirconium dioxide
NEMA grade G10	International Paper, Hampton, SC, USA	Dentin analog material – epoxy filled with woven glass fibers
Aquasil Easy Mix Putty and Aquasil Ultra Low Viscosity	Dentsply, Petropolis, RJ, Brazil	Hydrophilic addition reaction silicone
Porcelain conditioner	Dentsply, Petropolis, RJ, Brazil	10% hydrofluoric acid
Panavia F 2.0	Kuraray, Tokyo, Japan	Dual resin cement containing phosphate monomer (MDP)
Monobond S	Ivoclar Vivadent, Schaan, Liechtenstein	Silane coupling agent

2.2. Experimental test

The dies were fabricated with a dentin analog material (epoxy filled with woven glass fibers; NEMA grade G10). This material has elastic and adhesion properties similar to hydrated dentin [27]. The dimensions of the dies were described for the FEA models (Fig. 1). The restorations were made using the In-Ceram YZ system, which is a Y-TZP-based ceramic (YZ) SB veneered with a feldspathic porcelain (VM9) (Table 1). The experimental groups were divided ($n = 20$) according to the TOC angle of the preparation:

G6 – 6° TOC preparation and SB with uniform thickness (0.5 mm for the axial walls and 0.7 mm for the occlusal);
G12 – 12° TOC preparation and SB thickness as described for G6;
G20 – 20° TOC preparation and SB thickness as described for G6;

G20MOD – 20° TOC preparation and modified SB compensating the convergence, resulting in an external SB design similar to G6.

Fig. 2 schematically shows the preparation and SB design and the position and direction of load application for FEA and laboratory experiments. A representative die from each experimental group was duplicated in a type IV high-strength dental stone (CAM-base, Dentona AG, Dortmund, Germany). The dental stone dies were scanned by the CAD–CAM system (Cerec inLab, Sirona Dental Systems, Bensheim, Germany) and the substructures (SB) were generated by the software (inLab 2.9, Sirona). The G20MOD SB design was modified to increase the axial wall thickness compensating for the convergence angle and resulting in an external wall design similar to G6 SB. After machining, all SB were sonically cleaned in distilled water, subjected to the cleaning firing cycle (Table 3) and dipped in coloring liquid (Table 1) for 2 min, as per manufacturer's instructions. The substructures were sintered (Table 3) and a
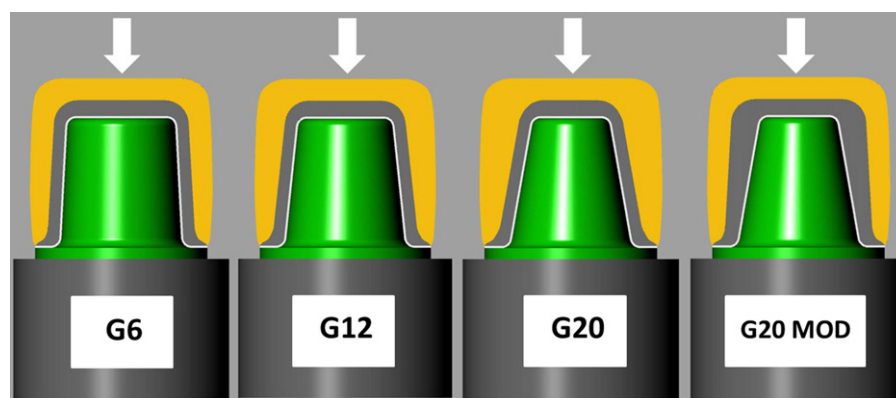
Fig. 2 – Schematic representation of the experimental groups: G6, G12, G20 and G20MOD. The external SB design of G20MOD is similar to G6, aiming to compensate for the convergence angle. The white arrows indicate the position and direction of the load application (on the center of the restorations, parallel to the long axis of the preparation). Ceramic SB (gray); porcelain (yellow); preparation (green). (For interpretation of the references to color in this figure legend, the reader is referred to the web version of this article.)

Table 2 – Elastic modulus (*E*) and Poisson's ratio (*υ*) values used for FEA models.		
Material	*E* (GPa)	*υ*
Y-TZP [8]	208	0.31
Feldspathic veneering porcelain [8]	67	0.21
Resin cement [31]	3.0	0.35
Dentin analog material [31]	14.9	0.31
Stainless steel [32]	200	0.3

laboratory technician applied the porcelain (VM9). First, a thin layer of porcelain was applied (wash) and sintered (Table 3), then the main porcelain layer (body) was applied to achieve the external design of the restoration, which was sintered in accordance with the manufacturer's instruction (Table 3). External wall standardization of the restorations was obtained using abrasive burs and controlled measurements (Digimatic caliper, Mitutoyo Corp., Tokyo, Japan), followed by a glaze cycle (Table 3). All restorations had a final thickness of 1.8 mm at the occlusal surface (SB – 0.7 mm; veneer – 1.1 mm) and 1.6 mm at the finish line (SB – 0.5 mm; veneer – 1.1 mm). The restoration thickness at the axial wall varied as described above. All restorations were sonically cleaned with isopropyl alcohol and cemented onto the woven glass fiber-filled epoxy dies using a resin cement system (Panavia F) containing a phosphate monomer (MDP) (Table 1). The bonding area of the dies were etched with 10% hydrofluoric acid for 1 min, washed in water, dried using oil-free air, silanated and the adhesive system (ED Primer A + B) was applied (Table 1) prior to cementation. Cement pastes were mixed and applied to the internal surface of the restorations, which were placed onto the dies. A constant cementation load of 750 g was applied to the occlusal surface and the excess cement was removed from the finishing line prior to light curing (Radii-cal LED curing light, SDI, Victoria, Australia; 1200 mW/cm^2) for 20 s from each restoration surface. The cemented restorations were stored in 37 °C distilled water for 24 h and randomly divided into two subgroups (*n* = 10): cyclic fatigued (c) or water stored.

To cyclic fatigue the restorations, the dies were hold by their base and submitted to 10^6 cycles at 4 Hz and load of 88 N (ERIOS ER-11000, São Paulo, Brazil) in 37 °C distilled water to simulate 1 year of oral service [33]. Cyclic fatigued restorations were inspected for surface damages under the stereomicroscope (Zeiss Stemi 2000-C, Edmund Optics Inc., Barrington, NJ, USA; 20–100×). The non-fatigued specimens were stored in 37 °C distilled water while the remaining specimens were cycled
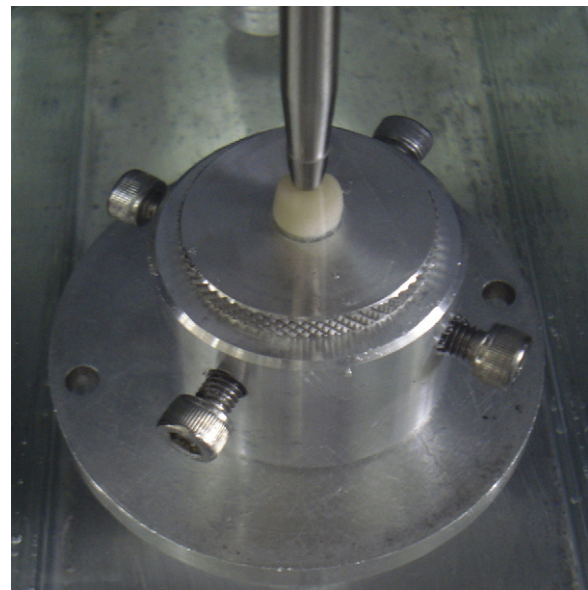

Fig. 3 – Image shows the piston applying a compressive load to the center of the occlusal surface of the restoration. "Crunch the crown" test used in this study.

fatigued (approximately 7 days). All restorations were submitted to a compressive load (crunch the crown test) applied by a sphere-shaped stainless steel piston (1.5 mm curvature radius) to the center of the occlusal surface (Fig. 3). The test was performed in a 37 °C water environment using a universal testing machine (EMIC DL-1000, EMIC, Sao Jose dos Pinhais, PR, Brazil) at a cross-head speed of 0.5 mm/min. The load to fracture (*L*, in N) was registered and the contact pressure (*P*) at fracture (MPa) was calculated according to the following equations [34,35]:

$$P = \left(\frac{3E_1}{4kr}\right)^{2/3} \frac{L^{1/3}}{\pi} \tag{1}$$

where *k* was obtained by the equation:

$$k = \frac{9}{16}[[1-(v)^2] + [1-(v_s)^2]]\frac{E}{E_s} \tag{2}$$

r is the curvature radius of the piston (1.5 mm), *v* is the Poisson's ratio of the surface subjected to the load (0.21), v_s is the

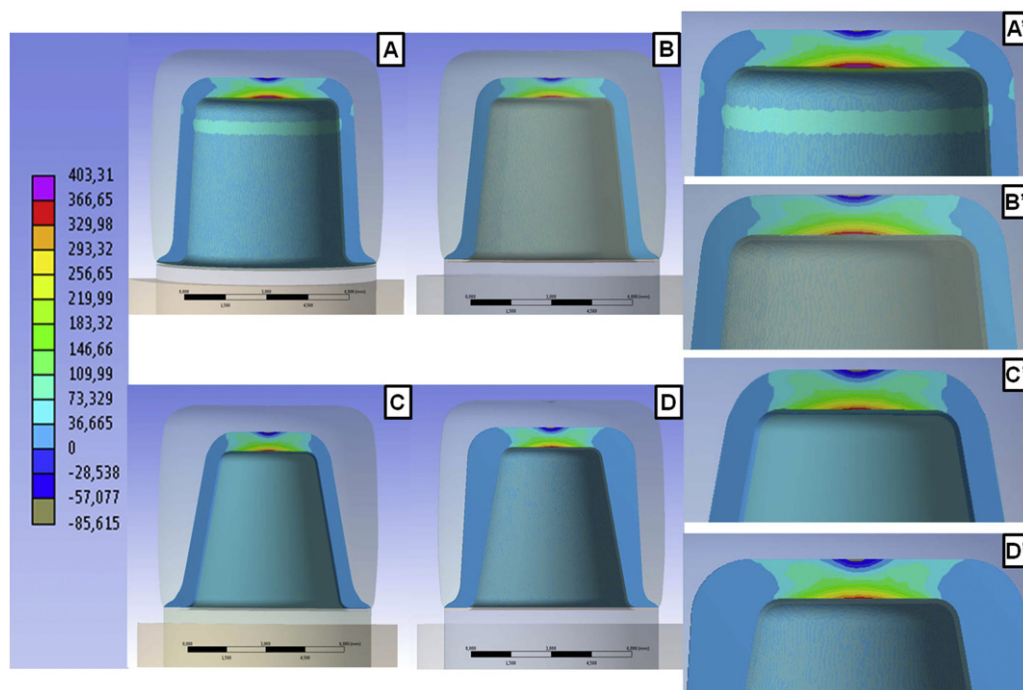| Table 3 – Parameters of the firing cycles used in this study during the fabrication of the restorations.						
Type of cycle	Furnace	Firing parameters				
		Starting temperature (°C)	Holding time (min)	Heating rate (°C/min)	Firing temperature (°C)	Holding time (min)
YZ sintering cycle	Zyrcomat T, Vita Zahnfabrik, Bad Sackingen, Germany	40	–	17	1530	120
YZ cleaning firing	Vacumat 6000 MP, Vita Zahnfabrik, Bad Sackingen, Germany	600	3	33	700	5
Base dentin wash firing		500	2	55	950	1
Body firing		500	6	55	910	1
Glaze firing		500	4	80	900	1

Fig. 4 – Stress distribution (MPS) in the ceramic SB (A: G6; B: G12; C: G20; D: G20MOD). A′, B′, C′ and D′ are close up views of the region with maximum stress (cementation surface) of G6, G12, G20 and G20MOD, respectively.

Table 4 – Mean, standard deviation (SD), load to fracture (L, in N) and contact pressure at fracture (P, in MPa) for each experimental group, including the cyclic fatigued (c) groups, and the statistical grouping.[a]				
Groups	n	L – mean (SD) (N)	P – mean (SD) (MPa)	Statistical grouping
G20MOD	10	2275 (417)	5449 (272)	A
G20MODc	10	2311 (538)	5397 (442)	A
G20	10	1693 (153)	4928 (98)	B
G20c	10	1694 (152)	4892 (146)	B
G12	10	1301 (145)	4436 (93)	C
G12c	10	1381 (179)	4601 (173)	C
G6	10	1432 (137)	4587 (83)	C
G6c	10	1483 (140)	4679 (151)	C

[a] Values followed by the same letter did not have statistically difference ($p \geq 0.05$).

Poisson's ratio of the piston (0.3), E is the elastic modulus of the surface subjected to the load (67 MPa), and E_s is the elastic modulus of the piston (200 MPa).

Fractographic principles were used to evaluate the fractured surfaces under a stereomicroscope (Zeiss Stemi 2000-C, Edmund Optics Inc., Barrington, NJ, USA) and a scanning electron microscope (MEV, JEOL Ltd., JSM 5600LV, Tokyo, Japan). The fracture origin and the failure modes were identified as chipping (porcelain fracture) or catastrophic failure (fracture of the porcelain and the substructure) [26].

Data were statistically analyzed using 2-way analysis of variance (ANOVA) and Tukey tests ($\alpha = 0.05$).

3. Results

The greatest MPS value in the porcelain was found for the G12 model (4839 MPa), followed by G20 (4267 MPa), G20MOD (3981 MPa) and G6 (3353 MPa). The pattern of stress distribution in the porcelain was similar for all evaluated models. Fig. 4 shows the FEA stress distribution for the different substructures considering the MPS. G6 transmitted the highest tensile stress values to the substructure (403 MPa) among all the groups (G12 – 389 MPa; G20 – 363 MPa; G20MOD – 351 MPa). The stress distribution in the SB showed a significant tensile stress concentration at the inner occlusal surface (cementation surface) for all models. G6 SB showed a ring-shaped area of low tensile stress value in the upper portion of the axial wall and a stronger tensile stress concentration in the cementation surface compared with the other groups.

All restorations showed no visible damage after cyclic fatigue. After loading, restorations failed by porcelain chipping or catastrophically. There was no case of die fracture. Data of load to failure (L) and contact pressure at fracture (P) are presented in Table 4.
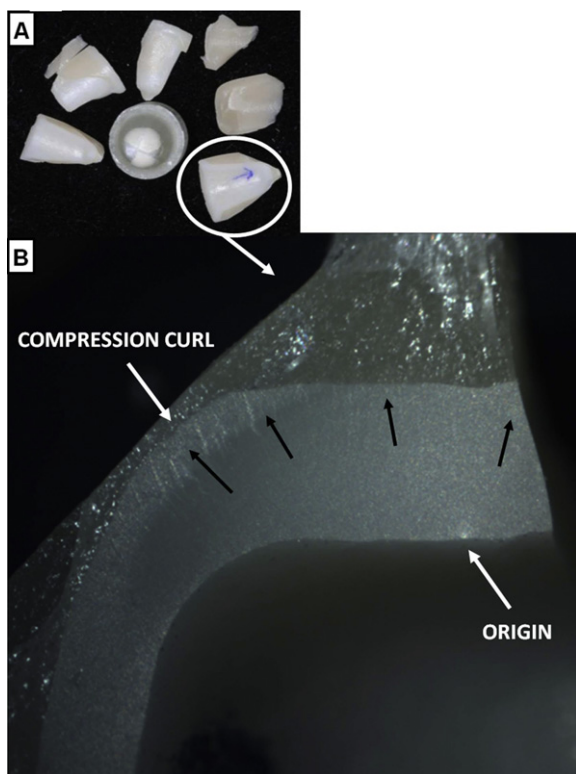
Fig. 5 – (A) Fragments from a catastrophic fractured specimen from G20; (B) stereomicroscopy image of the fractured surface containing the critical flaw (white arrow). Black arrows indicate the direction of crack propagation. The compression curl (white arrow) indicates the region of compressive stress.

The mean L and P values for the restorations in the G20MOD group were statistically greater than the mean values from other groups ($p = 0.000$). Cycling fatigue showed no statistical effect for each experimental model ($p = 0.44$). The lowest mean L and P values were found for G12 and G6 groups, which showed no statistical difference between them.

All chipping fractures (22.5%) initiated near the area of load application producing subsurface Hertzian cone cracks. When catastrophic failures (77.5%) occurred, the origin was located at the inner occlusal surface (cementation surface) of the substructure (Figs. 5 and 6).

Table 5 shows the number of catastrophic and chipping failures per experimental group and the mean load at fracture according to the failure mode. G6 specimens presented the highest number catastrophic failures (95%), which also prevailed in the restorations of G12 and G20.

4.   Discussion

As the aim of the present study was to investigate the influence of the tooth preparation TOC angle on the fracture load of Y-TZP based restorations, preparations and restorations were kept as simple as possible to avoid anatomical design interferences [36]. Yet, much effort was made to simulate the oral service, such as: using a dentin analog material to fabricate the

dies [27], using a resin bonding system that chemically bond to the zirconia-based ceramic [2,37], and a wet environment for cyclic fatigue and loading to fracture the restorations [2,38].

The maximum tensile stress values varied according to the FEA model: the greatest values were shown for G6 (403 MPa) and G12 (389 MPa), which restorations showed the lower load to fracture (Table 4). The restorations from the G20MOD showed the greatest load at fracture, followed by the restorations from the group with the same TOC angle preparation and standard SB (G20). Several factors could be associated with these results, including the occurrence of higher hoop stresses (circumferential stresses) with the reduction of convergence [39], which was suggested by the FEA model (Fig. 4A and A′). The elastic modulus (E) of the supporting substrate also influences the restoration fracture resistance, which increases as the E of the die increases [39], explaining the greater load to failure values of restorations tested on metal dies [40]. The present study used a dentin analog material.

Studies on the influence of porcelain thickness on the fracture resistance of restorations are controversial [9,11,12,41]. Yet, most of the studies showed that an increase in porcelain bulk is detrimental to the system behavior since it increases chipping [11,12]. Only one study reported no significant effect of porcelain thickness on the fracture resistance of restorations [41]. In the present study, the occlusal porcelain thickness, which was subjected to load application, was the same for all restorations. Nevertheless, the restorations from G20 had a greater bulk of porcelain in the axial area than the restorations from other groups, but it showed similar amount of chipping failures than G6 and G12 (Table 5). Perhaps the application of a non-center load could change the stress distribution and the system response [36]. Thus, the greatest values of load at fracture and contact pressure at fracture showed by the restorations from G20MOD are justified by SB strengthening due to the increased thickness of the SB, the decreased MPS in the SB, and a more uniform porcelain thickness [22,39].

Sitting the restorations from G6 was more difficult compared with the restorations from other groups because of the frictional resistance resulting from the TOC angle. Although the decrease in TOC angle increases the retention of restorations, there are limitations imposed by the frictional resistance, restoration strength, and the technical difficulties to perform parallel preparations [13–15,42]. Studies attempted to reproduce "ideal" convergence angles [16–19] and obtained mean TOC values between 14.1° [19] and 27.3° [16], suggesting the great difficulty to clinically achieve a 6° TOC angle preparation. It has been reported that preparations with 12° of TOC are ideal for CAD–CAM metal-free crowns [20,21]. Yet, as mentioned above, this convergence is difficult to achieve clinically. Therefore, considering these reports and the present study, it is recommended to follow the instructions from Shillingburg et al. [15], considering different TOC according to the type of tooth, indicating TOC angles of 24° mesiodistal, 20° buccolingual and 22° in general for mandibular first molars. Nevertheless, there is no data reporting on the effect of TOC angle on the retention of Y-TZP-based restorations.

Knowing the human bite force is important to design for the strength of restorative materials [43–46]. A study reported the mean maximum bite force of 847 N for men and 597 N for women in the molar region [45], which were similar to the

Table 5 – Classification according to the fracture type (chipping or catastrophic failure) in each experimental group, the mean value and standard deviation of the load at fracture (L, in N).

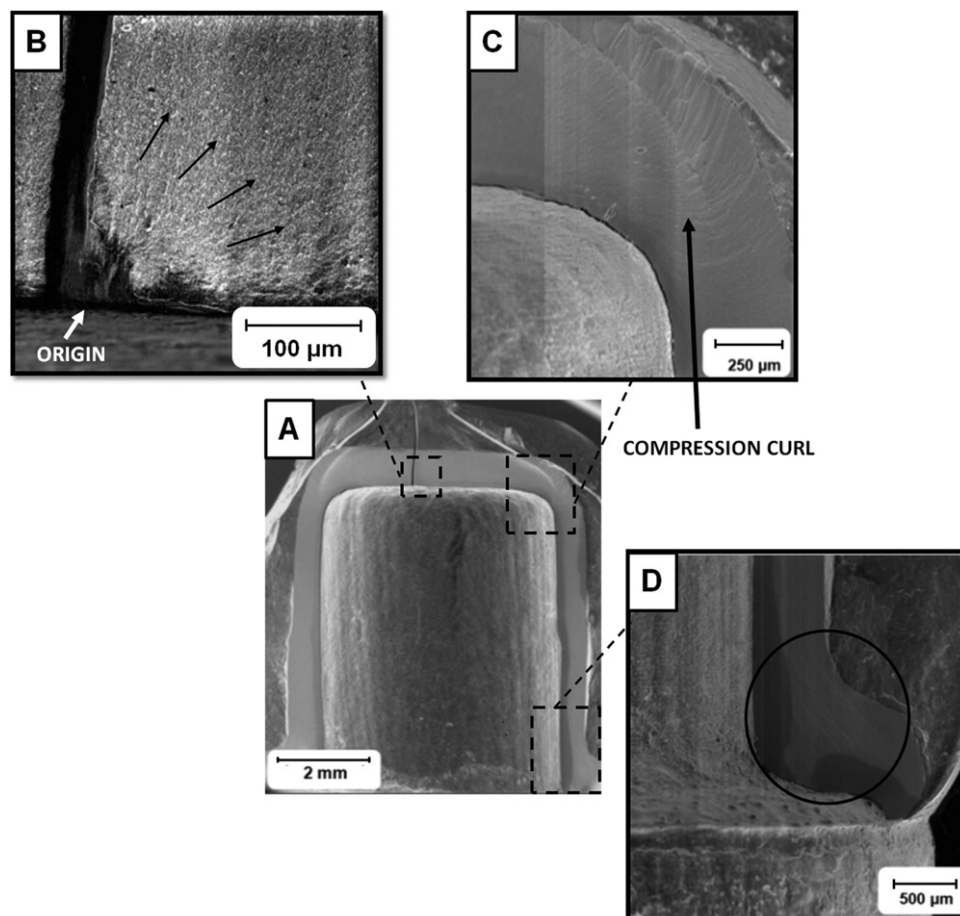|	Chipping		Catastrophic	
	Failures	L (N)	Failures	L (N)
G6	0	–	10	1395 (75)
G6c	1	1594	9	1471 (143)
Total	5%		95%	
G12	1	1385	9	1291 (151)
G12c	2	1246 (193)	8	1414 (172)
Total	15%		85%	
G20	3	1643 (40)	7	1714 (181)
G20c	0	–	10	1694 (152)
Total	15%		85%	
G20MOD	5	2576 (326)	5	1974 (243)
G20MODc	6	2712 (127)	4	1710 (195)
Total	55%		45%	

Fig. 6 – Photomicrographs (SEI) of a fractured restoration (G6). (A) Global view of a fractured fragment on the die (34×), (B) fracture origin at higher magnification (782×). The black arrows indicate the direction of the crack propagation (dcp); (C) black arrow indicates the compression curl (200×), (D) black circle contains some wake hackles that confirmed the dcp (100×).

mean value (580 N) of another study [46]. In the present study the mean load at fracture values ranged from 1301 N (G12) to 2311 N (G20MODc), which are greater than the mean maximum human bite force. Yet, the bite force is distributed among several occlusal contact points that can vary in size and number, resulting in a contact pressure value on each site of load application. Therefore, the contact pressure at fracture (P) is other important information to understand the behavior of restorative materials [47]. These authors [47] found maximum human bite forces ranging from 1042 N to 1650.8 N, occlusal contact areas between 28.2 mm^2 and 47.7 mm^2, and contact pressure values from 35.1 MPa to 42.3 MPa. Considering only the molar region, these authors [47] found a mean maximum force ranging from 410 N to 630 N distributed in areas from 10 mm^2 to 18 mm^2, and resulting in mean pressure between 35 MPa and 43 MPa. In the present study the mean P values ranged from 4436 MPa (G12) to 5449 MPa (G20MOD), which are again much greater than the physiological human P values that rarely exceeds 43 MPa [47].

Cyclic fatigue simulating 1 year of oral service showed no effect on the load to fracture of restorations from same experimental design. Clinical studies with zirconia-based ceramic restorations have showed that chipping is the most common failure mode [23,24,48]. In the present study, most restorations failed catastrophically (77.5%), which may be explained by the type and location of load application, meaning, one centered occlusal point of contact pressure, and the ceramic to resin bond on a dentin analog die. In addition, previous studies suggested an inadequate wettability of the porcelain on the zirconia-based SB that was recently improved by the use of the coloring liquid [8], recommended by the manufacturer and used in the present study. Fractographic analyses of the fractured restorations showed the origin location in the inner occlusal surface (Figs. 5 and 6), which is an area of greater tensile stresses during loading (Fig. 4), in agreement with previous findings [27]. Yet, the catastrophic failures always showed some porcelain chipping initiating from the area of load application, and producing an "onion-like" aspect because of chipping of porcelain layers that progressed from Hertzian cone cracks, in agreement with previous reports [11,12,28]. All chipping only fractures (22.5%) initiated near the area of load application producing subsurface Hertzian cone cracks, as previously reported [6]. Thus, considering that this study did not reproduce a typical physiological occlusal load, the fracture modes resulted from the experimental restorations are similar to the ones previously reported. Yet, fractography of clinically failed restorations should provide the best information on the possible modes of failure.

5.   Conclusions

Despite of a similar stress distribution, different MPS values were shown for the FEA models, confirming the first study hypothesis. The lowest MPS value was generated in the SB of the G20MOD FEA model, suggesting a superior mechanical behavior, which was confirmed experimentally.

The parameters used for the cyclic fatigue had no significant influence on the fracture load of restorations of same design, rejecting the second study hypothesis.

The TOC angle of the preparation and the SB design influenced the load to fracture the Y-TZP-based ceramic restorations, confirming the third study hypothesis. Restorations from G20MOD group showed the greatest load to fracture. Regardless of the preparation TOC, the YZ–VM9 restorations showed greater load to fracture than the reported physiological occlusal load.

REFERENCES

[1] Kelly JR, Denry I. Stabilized zirconia as a structural ceramic: an overview. Dental Materials 2008;24: 289–98.

[2] Della Bona A. Bonding to ceramics: scientific evidences for clinical dentistry. São Paulo: Artes Médicas; 2009.

[3] Sundh A, Molin M, Sjögren G. Fracture resistance of yttrium oxide partially stabilized zirconia all-ceramic bridges after veneering and mechanical fatigue testing. Dental Materials 2005;21:476–82.

[4] Della Bona A, Donassollo TA, Demarco FF, Barrett AA, Mecholsky Jr JJ. Characterization and surface treatment effects on topography of a glass-infiltrated alumina/zirconia-reinforced ceramic. Dental Materials 2007;23:769–75.

[5] Pittayachawan P, McDonald A, Young A, Knowles JC. Flexural strength, fatigue life, and stress-induced phase transformation study of Y-TZP dental ceramic. Journal of Biomedical Materials Research Part B: Applied Biomaterials 2009;88:366–77.

[6] Swain MV. Unstable cracking (chipping) of veneering porcelain on all-ceramic dental crowns and fixed partial dentures. Acta Biomaterialia 2009;5:1668–77.

[7] Kim JW, Covel NS, Guess PC, Rekow ED, Zhang Y. Concerns of hydrothermal degradation in CAD/CAM zirconia. Journal of Dental Research 2010;89:91–5.

[8] Borba M, de Araújo MD, de Lima E, Yoshimura HN, Cesar PF, Griggs JA, et al. Flexural strength and failure modes of layered ceramic structures. Dental Materials 2011;27:1259–66.

[9] Doyle MG, Munoz CA, Goodacre CJ, Friedlander LD, Moore BK. The effect of tooth preparation design on the breaking strength of Dicor crowns: 2. International Journal of Prosthodontics 1990;3:241–8.

[10] Goodacre CJ, Campagni WV, Aquilino SA. Tooth preparations for complete crowns: an art form based on scientific principles. Journal of Prosthetic Dentistry 2001;85:363–76.

[11] Rosentritt M, Steiger D, Behr M, Handel G, Kolbeck C. Influence of substructure design and spacer settings on the in vitro performance of molar zirconia crowns. Journal of Dentistry 2009;37:978–83.

[12] Bonfante EA, Rafferty B, Zavanelli RA, Silva NR, Rekow ED, Thompson VP, et al. Thermal/mechanical simulation and laboratory fatigue testing of an alternative yttria tetragonal zirconia polycrystal core–veneer all-ceramic layered crown design. European Journal of Oral Sciences 2010;118:202–9.

[13] Parker MH, Calverley MJ, Gardner FM, Gunderson RB. New guidelines for preparation taper. Journal of Prosthodontics 1993;2:61–6.

[14] Wilson Jr AH, Chan DC. The relationship between preparation convergence and retention of extracoronal retainers. Journal of Prosthodontics 1994;3:74–8.

[15] Shillingburg HT, Hobo S, Whitsett LD, Jacobi R, Brackett SE. Fundamentals of fixed prosthodontics. Tokyo: Quintessence; 2007.

[16] Leempoel PJ, Lemmens PL, Snoek PA, van't Hof MA. The convergence angle of tooth preparations for complete crowns. Journal of Prosthetic Dentistry 1987;58:414–6.

[17] Nordlander J, Weir D, Stoffer W, Ochi S. The taper of clinical preparations for fixed prosthodontics. Journal of Prosthetic Dentistry 1988;60:148–51.

[18] Smith CT, Gary JJ, Conkin JE, Franks HL. Effective taper criterion for the full veneer crown preparation in preclinical prosthodontics. Journal of Prosthodontics 1999;8:196–200.

[19] Ayad MF, Maghrabi AA, Rosenstiel SF. Assessment of convergence angles of tooth preparations for complete crowns among dental students. Journal of Dentistry 2005;33:633–8.

[20] Beuer F, Edelhoff D, Gernet W, Naumann M. Effect of preparation angles on the precision of zirconia crown copings fabricated by CAD/CAM system. Dental Materials Journal 2008;27:814–20.

[21] Beuer F, Aggstaller H, Richter J, Edelhoff D, Gernet W. Influence of preparation angle on marginal and internal fit of CAD/CAM-fabricated zirconia crown copings. Quintessence International 2009;40:243–50.

[22] De Jager N, Pallav P, Feilzer AJ. The influence of design parameters on the FEA-determined stress distribution in CAD–CAM produced all-ceramic dental crowns. Dental Materials 2005;21:242–51.

[23] Raigrodski AJ, Chiche GJ, Potiket N, Hochstedler JL, Mohamed SE, Billiot S, et al. The efficacy of posterior three-unit zirconium-oxide-based ceramic fixed partial dental prostheses: a prospective clinical pilot study. Journal of Prosthetic Dentistry 2006;96:237–44.

[24] Sailer I, Fehér A, Filser F, Gauckler LJ, Lüthy H, Hämmerle CH. Five-year clinical results of zirconia frameworks for posterior fixed partial dentures. International Journal of Prosthodontics 2007;20:383–8.

[25] Ereifej N, Rodrigues FP, Silikas N, Watts DC. Experimental and FE shear-bonding strength at core/veneer interfaces in bilayered ceramics. Dental Materials 2011;27:590–7.

[26] Quinn GD. Fractography of ceramics and glasses. Washington: Natl. Inst. Stand. Technol.; 2007, 4/1-4/46.

[27] Kelly JR, Rungruanganunt P, Hunter B, Vailati F. Development of a clinically validated bulk failure test for ceramic crowns. Journal of Prosthetic Dentistry 2010;104:228–38.

[28] Silva NR, Bonfante EA, Rafferty BT, Zavanelli RA, Rekow ED, Thompson VP, et al. Modified Y-TZP core design improves all-ceramic crown reliability. Journal of Dental Research 2011;90:104–8.

[29] Anusavice KJ, Kakar K, Ferree N. Which mechanical and physical testing methods are relevant for predicting the clinical performance of ceramic-based dental prostheses? Clinical Oral Implants Research 2007;18:218–31.

[30] Mou SH, Chai T, Wang JS, Shiau YY. Influence of different convergence angles and tooth preparation heights on the internal adaptation of Cerec crowns. Journal of Prosthetic Dentistry 2002;87:248–55.

[31] Yi YJ, Kelly JR. Effect of occlusal contact size on interfacial stresses and failure of a bonded ceramic: FEA and monotonic loading analyses. Dental Materials 2008;24: 403–9.

[32] Necchi S, Taschieri S, Petrini L, Migliavacca F. Mechanical behaviour of nickel–titanium rotary endodontic instruments in simulated clinical conditions: a computational study. International Endodontic Journal 2008;41:939–49.

[33] Wiskott HW, Nicholas JL, Belser UC. Stress fatigue: basic principles and prosthodontic implications. International Journal of Prosthodontics 1995;8:105–16.

[34] Kelly JR. Clinically relevant approach to failure testing of all-ceramic restorations. Journal of Prosthetic Dentistry 1999;81:652–61.

[35] Kelly JR, Benetti P, Rungruanganunt P, Bona AD. The slippery slope – critical perspectives on in vitro research methodologies. Dental Materials 2012;28:41–51.

[36] Rekow ED, Harsono M, Janal M, Thompson VP, Zhang G. Factorial analysis of variables influencing stress in all-ceramic crowns. Dental Materials 2006;22: 125–32.

[37] de Oyagüe RC, Monticelli F, Toledano M, Osorio E, Ferrari M, Osorio R. Influence of surface treatments and resin cement selection on bonding to densely-sintered zirconium-oxide ceramic. Dental Materials 2009;25:172–9.

[38] Della Bona A, Anusavice KJ, DeHoff PH. Weibull analysis and flexural strength of hot-pressed core and veneered ceramic structures. Dental Materials 2003;19:662–9.

[39] Scherrer SS, de Rijk WG. The fracture resistance of all-ceramic crowns on supporting structures with different elastic moduli. International Journal of Prosthodontics 1993;6:462–7.

[40] Cho L, Song H, Koak J, Heo S. Marginal accuracy and fracture strength of ceromer/fiber-reinforced composite crowns: affect of variations in preparation design. Journal of Prosthetic Dentistry 2002;88:388–95.

[41] Webber B, McDonald A, Knowles J. An in vitro study of the compressive load at fracture of Procera AllCeram crowns with varying thickness of veneer porcelain. Journal of Prosthetic Dentistry 2003;89:154–60.

[42] Bowley JF, Kieser J. Axial-wall inclination angle and vertical height interactions in molar full crown preparations. Journal of Dentistry 2007;35:117–23.

[43] Howell AH, Manly RS. An electronic strain gauge for measuring oral forces. Journal of Dental Research 1948;27:705–12.

[44] Anderson DJ. Measurement of stress in mastication. Journal of Dental Research 1956;35:664–70.

[45] Waltimo A, Könönen M. A novel bite force recorder and maximal isometric bite force values for healthy young adults. Scandinavian Journal of Dental Research 1993;101:171–5.

[46] Tortopidis D, Lyons MF, Baxendale RH, Gilmour WH. The variability of bite force measurement between sessions, in different positions within the dental arch. Journal of Oral Rehabilitation 1998;25:681–6.

[47] Shinogaya T, Bakke M, Thomsen CE, Vilmann A, Sodeyama A, Matsumoto M. Effects of ethnicity, gender and age on clenching force and load distribution. Clinical Oral Investigations 2001;5:63–8.

[48] Della Bona A, Kelly JR. The clinical success of all-ceramic restorations. Journal of the American Dental Association 2008;139:8S–13S.